14. E. É. Zasimchuk and S. I. Selitser, Metallofizika, 9, No. 3, 44-47 (1987).
15. J. Friedel, Dislocations, Pergamon Press, New York (1964).
16. J. P. Hirth and J. Lothe, Theory of Dislocations, McGraw-Hill, New York (1967).
17. L. D. Landau and E. M. Lifshitz, Hydrodynamics: Theoretical Physics [in Russian], Vol. 6, Nauka, Moscow (1988).

REGULARITIES OF SUBSTRUCTURAL HARDENING

N. A. Koneva and É. V. Kozlov

UDC 539.3:669.7.017

INTRODUCTION

There exist four basic mechanisms of resistance of plastic deformation of metallic materials: 1) lattice (Peierls–Nabarro forces, the restructuring of the dislocation core, electron and phonon retardation etc.); 2) solid-solution; 3) substructural; 4) polyphasic (dispersed, composite). As analyses of recent years have shown, hardening caused by radiative and tempering defects, reduces to the action of the enumerated mechanisms. Substructural hardening is an extremely important mechanism of hardening of metals and alloys. It controls deformation hardening and contributes significantly to the strength of materials of the martensitic class. Hardening caused by different forms of thermomechanical treatment also basically is incumbent upon substructural hardening. Finally, both the origin and development of microfissures is tightly connected with substructure evolution.

The nature of substructural hardening has been experimentally and theoretically analyzed over the course of several decades [1-4]. Undoubtedly, retardation of slippage caused by dislocated structures depends on the location of dislocations, that is, on the type of substructure [5]. However, in far from all the papers, in analyzing substructural hardening, has the nature of the location of dislocations been brought to attention [3, 4, 6].

The authors of this paper have in the last ten years been developing a concept of substructural hardening, at the basis of which lies the distinguishing of characteristic types of substructure, differing in the physical nature of formation of shearing strength. This article contains a description of the present state of the problem. It develops concepts laid out in the preceding survey of Koneva and Kozlou [7], however it does not repeat the material of that publication. Hardening caused by the effect of polycrystallization, undoubtedly pertains to the substructure, but on a higher structural level (see the classification of structural levels in [8]). The contemporary state of polycrystalline hardening has been illuminated in a series of papers by Koneva, Sharkeev, et al. [10], and here, due to insufficient space, is not considered.

1. BRIEF CLASSIFICATION OF SUBSTRUCTURES

A classification of dislocated substructures observed in deformed materials, was presented in detail in a recent survey of Koneva and Kozlov [8]. In considering substructural hardening, it is necessary to distinguish [12, 13] homogeneous nondisoriented substructures (dislocation chaos, accumulation, recticular substructure), inhomogeneous nondisoriented (dislocated concentrations, balls, cells, cellular-recticular substructure), disoriented dislocation-disclination (disoriented cells, disoriented cellular-reticular, band and substructure with continuous and discrete disorientations or oriented chaos), disoriented dislocation-free (subgranular or fragmented), disoriented twin and martensitic (multilayered packing defects, twins of deformation, deformed martensite).

In subsequent consideration, it is necessary to emphasize the following three features of inhomogeneous and disoriented substructures of a deformed origin. Firstly, there are encountered in them different local dislocated configurations, namely: chaotic concentrations of dislocations, ordered dislocated balls, boundaries of cells with a dipolar configuration not introduced by disorientation, and boundaries of cells with a surplus of dislocations of one sign, introduced by disorientation (Fig. 1a-c). Secondly, subboundaries of

Tomsk Engineering-Structural Institute. Translated from Izvestiya Vysshikh Uchebnykh Zavedenii, Fizika, No. 3, pp. 56-70, March, 1991.

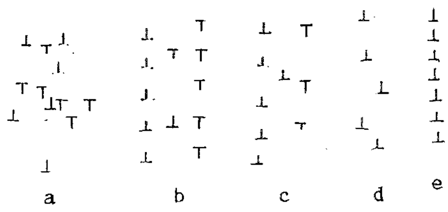

Fig. 1. Basic types of dislocated configurations lying at the basis of the classification of inhomogeneous and disoriented substructures; a) concentrations; b and c) walls of cells without disorientation and with disorientation, respectively; d) subboundaries; e) boundaries of fragments. Besides the boundaries of the fragments, all the remaining configurations are depicted by imperfect ones.

a different degree of perfection and boundaries of fragments (Fig. 1d, e). Formations of the first and second types can be both closed and ragged. Each of the features enumerated above determines by its presence a corresponding type of substructure. Finally, the third feature, distributed dislocated charges, occupying the entire volume of the material or a part of it, is characteristic for disoriented substructures. They introduce a continuous curvature-torsion ($\varkappa$) of the crystal lattice and its gradient ($\partial\varkappa/\partial\ell$).

2. CONNECTION OF THE FLOW STRESS σ WITH THE MEAN SCALAR DENSITY OF DISLOCATIONS ρ

We have the well-known relation

$$\sigma=\sigma_f+m\alpha Gb\rho^{1/2}, \tag{1}$$

where α is a parameter characterizing the shearing strength; G is the shear modulus; b is Burgers vector; σ_f is the total contribution of lattice and solid-solution hardening. Experimental data of the last decade show that the parameter α determining the shearing strength depends on the type of the substructure [14, 15]. Since, in the process of evolution of the defect structure, there ususally are present in the volume of the frame two different substructures [8] and the ratio of the volumetric shares is nonconstant, the dependence $\sigma = f(\rho^{1/2})$, as a rule, has a nonlinear nature [7, 12, 16]. In the general case, taking into account sequentially changing substructures in the course of plastic deformation in a wide interval of dislocation density, the dependence $\sigma = f(\rho^{1/2})$ can be represented in the form of a scheme (Fig. 2), which is composed by taking into account all the results obtained by the authors with collaborators on different materials. In the stage of nondisoriented substructures (part 1) the dependence of $\sigma = f(\rho^{1/2})$ is close to linear. The appearance of disoriented substructures and especially band substructure (part 2) leads to the growth of the coefficient α, in the stage of oriented chaos (part 3) the parameter α again decreases somewhat (it is necessary to keep in mind that in the case of experiments with polycrystalline frames, as a rule, the joint parameter $m\alpha$ is determined). When the perfected fragmented substructure is sufficiently developed, the density of dislocations diminishes [17], and the increase of flow stress is caused here by the increase of density of the boundaries of the fragments (Fig. 2a, branch 4). An additional contribution $\Delta\sigma$ to the flow stress caused by the appearance of disorientations, both discrete and smooth, can be evaluated

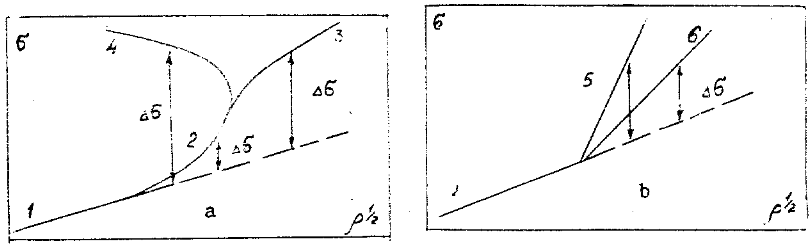

Fig. 2. Form of the dependence of σ–$\rho^{1/2}$ for different classes of substructures. Shown are ways to determine the contribution $\Delta\sigma$, caused by the introduction of continuous and discrete disorientations of different type.

TABLE 1

Type of substructure				Material: polycrystals Cu—Al, Cu—Mn	monocrystals [001] Ni	monocrystals [001] Ni—Fe, Ni—Fe—Cr	polycrystals Ni—Fe, Ni—Fe—Cr	polycrystals Fe—Mn
Nondisoriented	Homogeneous	Dislocated	Chaos			0,4	1,5—2,0	
Nondisoriented	Homogeneous	Dislocated	Meshes	2,5—5,0		1,0	1,5	
Nondisoriented	Inhomogeneous	Dislocated	Balls			1,4	2,2	
Nondisoriented	Inhomogeneous	Dislocated	Cells	2,5—3,0	0,05	2,5	3,0	1,5
Disoriented	Inhomogeneous	Dislocated	Cellular-mesh	7,5—8,0		2,5	1,8—2,2	
Disoriented	Inhomogeneous	Dislocation-disclination	Band	6,5—13,0	1,0	5,0—5,5	3,5—6,5	
Disoriented	Inhomogeneous	Dislocation-disclination	Oriented chaos			1,5—3,2	1,5—2,8	
Disoriented	Inhomogeneous	Dislocation-disclination	Fragmented				from +3,0 to −1,5 across ∓∞	
Disoriented	Inhomogeneous	Twin and martensitic	Twin	17—25			8	2,5
Disoriented	Inhomogeneous	Twin and martensitic	Martensitic				10—14	

as the difference of the extrapolated linear part and the corresponding branches of the dependence $\sigma = f(\rho^{1/2})$. In the case of the formation of deformation twins (branch 5) and martensite (branch 6) the boundaries of the division and disorientations introduced by them also lead to the growth of α (Fig. 2b).

The characteristic magnitudes of the parameter $m\alpha$ for different substructures of fcc-metals and solid solutions are represented in Table 1. In analyzing the values of $m\alpha$ it is most important to bring to attention their relative change during the change of the substructure, and not really the absolute values. The situation is that the latter still depend on the type of crystal lattice, the presence of admixtures in the metal or concentration of the solid solution, the texture of the polycrystals or the orientation of the monocrystals, the number of active slippage systems, the state of order in the solid solution, the temperature of the experiment, etc.

So, for example, in monocrystals of the alloy Ni_3Fe, the parameter α is maximal along the line [001] − [$\bar{1}$11] of the basic stereographic triangle, decreasing in this same direction. A subsequent decrease of the parameter α is observed in displacing the deformation axis through the center of the stereographic triangle to the vertex [011]. In the ordered alloys, the parameter α decreases with a lowering of the degree of the distant atomic order [18]. In pure metals, this parameter, as a rule, is less than in solid solutions; moreover, for metals with a bcc lattice, it is usually somewhat less than for metals with a fcc lattice. The influence of changing the type of substructure is similar in different materials. So, in any materials under any conditions of deformation, the transition from nondisoriented substructures to disoriented ones leads to an increase of α (or $m\alpha$, where m is the orientation factor).

The nature of the dependence of $\sigma = f(\rho^{1/2})$ for nondisoriented substructures was discussed in our earlier papers [7, 12, 14, 16, 19]. It was established that for reticular and cellular-reticular substructures, there is a linear relation, and for a ball-cellular substructure, a noticeable departure from linear dependence is observed. Experimental data on the behavior of the dependence of $\sigma = f(\rho^{1/2})$ in the formation of disorientations are presented below in considering specific substructures.

3. INFLUENCE OF SUBSTRUCTURE ON THE ACCUMULATION OF DEFECTS, SLIPPAGE CHARACTERISTICS, AND ANNIHILATION OF DISLOCATIONS

The type of substructure determines the majority of characteristics of a deformable meterial. It is known that the phasic nature of deformed hardening is caused by the sequential change of substructures [8]. The deformation hardening coefficient $\Theta = d\sigma/d\varepsilon$ is maximal in the stage of nondisoriented substructures, and the dependence of the flow stress on the deformation $\sigma = f(\varepsilon)$ here has a character close to linear (Fig. 3a). Parabolic hardening is observed in the formation of disoriented substructures [12, 15, 20-26].

The slippage picture depends on the type of substructure [27]. Highly homogeneous narrow slippage is observed in the base of ball-cellular nondisoriented substructures. The transition to reticular substructures increases slippage localization. Subsequent growth of slippage localization occurs during the formation of disoriented substructures, which is accompanied simultaneously by the appearance of kink bands, reorientation, and distortion of the slippage planes.

The velocity of accumulation of the scalar density of dislocations $d\rho/d\varepsilon$ is maximal in the phase of nondisoriented substructures and sharply decreases in the transition to disoriented (Fig. 3a) [12, 23-30]. On the contrary, the velocity of accumulation of the excess dislocation density $d\rho_{\pm}/d\varepsilon$ in moderately and strongly deformed materials is proportional to the curvature-torsion of the crystal lattice $\varkappa = b\rho_{\pm}$) attains a maximum during the formation of the band substructure and then decreases in the transition to oriented chaos (Fig. 3a). During the formation of the fragmented substructure, the velocity of accumulation of dislocations does not simply decrease, and can pass through zero and change its sign if highly perfect fragments are formed. The origin of disoriented substructures is connected with the sharp growth of the process of annihilation of dislocations (Fig. 3b) [12, 24, 27].

The inhomogeneity of the local characteristics of the dislocated structure also depends on its type. For example, the gradient of the continuous curvature-torsion of the crystal lattice $\partial\varkappa/\partial\ell$ is not great in nondisoriented substructures and sharply increases in passing to a band substructure and especially to a substructure with continuous and discrete disorientations (Fig. 3b) [20]. In passing to a fragmented substructure and its perfection, the values of $\varkappa$ and $\partial\varkappa/\partial\ell$ decrease.

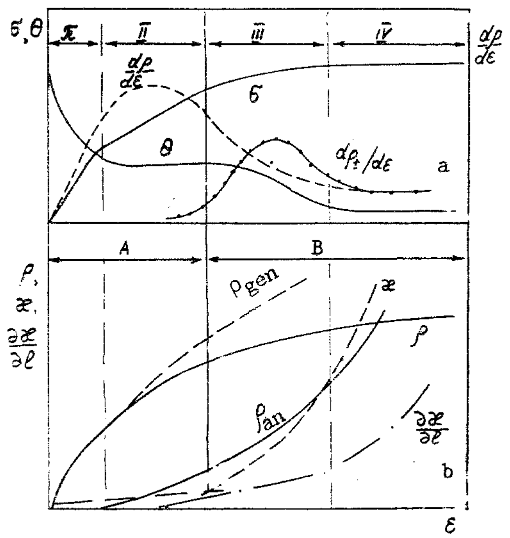

Fig. 3. Influence of the type of substructure on the parameters of defect-formation and the phasic nature of the curve of flow [8, 20]. Dependences are shown on the degree of deformation of the flow stress σ, the hardening coefficient Θ, the density of dislocations ρ in the material and the annihilated dislocations ρ_{an}, all the dislocations participating in the deformation, ρ_{gen}, the velocities of accumulation of the scalar $d\rho/d\varepsilon$ and excess $d\rho\pm/d\varepsilon$ density of dislocations, the curvature-torsion of the crystal lattice $\varkappa$ and its gradient $\partial\varkappa/\partial\ell$. A and B are the regions of nondisoriented and disoriented substructures, respectively; π, II, III, IV are the names of the transitional and II etc. of the deformation phases.

4. HARDENING FEATURES IN DIFFERENT SUBSTRUCTURES

In the previous survey of Kareva and Kozlov [7] there was considered, basically, hardening in nondisoriented substructures — reticular and cellular. In recent years, considerable information has been accumulated on the influence of discrete and continuous disorientations on hardening; furthermore, regularities of the hardening of disoriented substructures have been studied in detail. Below is sequentially considered the connection of the flow stress with the parameters of different substructures.

Reticular Substructure. Here the basic mechanism of slippage retardation, as was established earlier [7, 14, 32, 33], is the retardation of individual dislocations on thresholds, reactions and dislocation barriers. Displacement retardation is carried out along the entire slippage plane, practically for each dislocation. This also is a contact retardation. Shearing strength is proportional to the density of these obstacles (Fig. 4). It is evident that the effectiveness of the retardation depends on the orientation of the monocrystals. The contribution of the long-range stress fields in this substructure behaves quite peculiarly [14, 34]. The residual stresses, measured along the radius of the bend of the dislocations (see the method in [35, 36]), immediately after the limit of fluidity, comprise not less than half of the active stresses τ, and to the end of existence of the reticular substructure, this contribution decreases to 1/3 from τ.

Cellular-reticular Substructure. Retardation of displacement in this substructure has an intermediate character between that of contact, as in reticular, and barrier, as in cellular. On one hand, the flow stress is inversely proportional to the distance between the dislocated concentrations (Fig. 5a), and on the other, the shearing strength grows proportionally to $\rho_{cr}^{1/2}$, where ρ_{cr} is the density of dislocations in the concentrations (Fig. 5b).

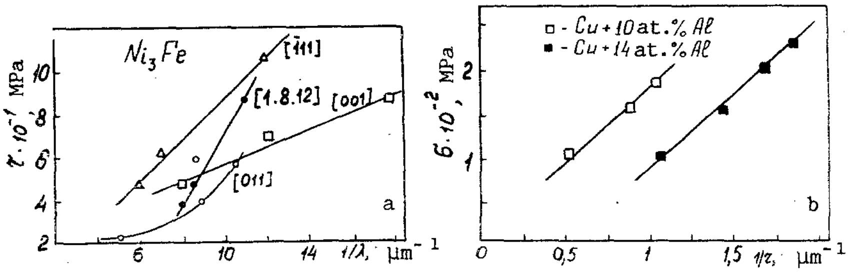

Fig. 4. Dependence of shearing strength on the density of obstacles ($1/\lambda$) along the lines of dislocations (a) and flow stress (σ) on the density ($1/r$) of dislocation barriers (b); a are monocrystals of Ni_3Fe of different orientations; b are polycrystals of the alloys Cu—Al.

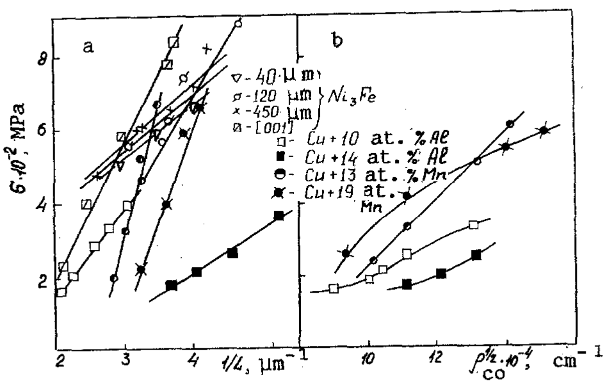

Fig. 5. Role of barrier (a) and contact (b) retardation in the formation of flow stress (σ) in a cellular-reticular substructure: polycrystals of disordered alloy Ni_3Fe (a) with different dimension of grains, monocrystals [001] of this same alloy and polycrystals of the alloys Cu—Al and Cu—Mn (b).

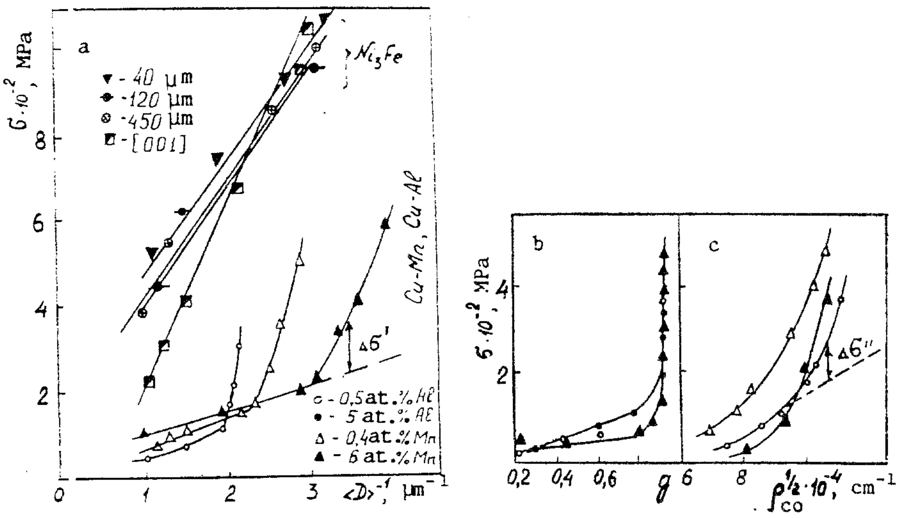

Fig. 6. Dependence of the flow stress on the parameters of the cellular substructure. The ordered alloy Ni_3Fe (the monocrystals [001] and the polycrystals with different dimension of grains) and polycrystals of the alloys Cu–Al and Cu–Mn.

Cellular Substructure. In a cellular substructure, the role of barrier retardation of displacement grows [7, 14, 27]. In distinction from contact retardation, barrier retardation is carried out not along the entire slippage plane, but is localized on dislocated concentrations of a different type (see Fig. 1). The flow stress here is inversely proportional to the dimension (D) of the cells (Fig. 6a). A similar dependence has been described in papers of various authors [37, 38]. With the appearance of disorientations, the slope of $\sigma = f(D^{-1})$ changes. With the growth of perfection of the cellular structure – with respect to the share of the closed boundaries of the cells g – the flow stress grows. Experimental data show that the dislocations inside the cells do not control the flow stress. However, the presence of contact retardation of displacement on dislocations in the walls of the cells is obvious (Fig. 6c): the flow stress is proportional to the square root of the density of dislocations in the walls of the cells (ρ_{wa}). A similar dependence was described in [39]. A sufficiently sharp break is observed in the dependences of the flow stresses on D^{-1} and $\rho_{wa}{}^{1/2}$ for copper alloys, caused by the change to a disoriented cellular substructure. In Fig. 6 it is shown how by extrapolation one can determine the contributions $\Delta\sigma'$ and $\Delta\sigma''$ caused by the disorientation. The first of them determines an additional contribution to the flow stress in passing from a nondisoriented cellular structure to a disoriented one, and the second – the increase of the effectiveness of retardation in the walls of cells during the appearance in them of excess dislocated charge (in Fig. 1 this is the transition from case b to case c).

An important factor also controlling the flow stress in a cellular substructure is (Fig. 6b) the degree of closure of the boundaries of the cells (g is the ratio of the number of closed cells to their overall number). According to the measure of perfection of the cellular substructure, the shearing strength grows.

As has alrady been noted, the transition to disoriented substructures increases the effectiveness of the obstacles, retarding the slippage. For a cellular substructure, the role of this factor has been studied in detail in our papers. With the increase of the density of disoriented boundaries of the cells $P_{d.bo}$ (these are the boundaries on which the discrete disorientation φ exceeds 0.5°) the flow stresses grow linearly (Fig. 7a). The sharp bend in the dependences $\sigma = f(P_{d.bo})$ is connected with the appearance of boundaries of the band substructure. The flow stresses grow also with the increase of the disorientation angle φ. Especially well-apparent is the increase of the effectiveness of the boundaries of the cells as barriers to slippage with the growth of the disorientation angle, if the additional contribution $\Delta\sigma'$ is represented as the function φ (Fig. 7b). In correspondence with the prediction of the theory (see, for example, [5]), for small angles there is a linear dependence $\Delta\sigma' = f(\varphi)$, that is, in fact, observed experimentally (Fig. 7c). If one represents the contributions $\Delta\sigma'$ and $\Delta\sigma''$ depending on the density of disoriented boundaries of the cells, then increasing dependences, close to linear, are uncovered. In such a manner, one has succeeded in precisely distinguishing the influence of disorientation on the shearing strength in cellular substructure.

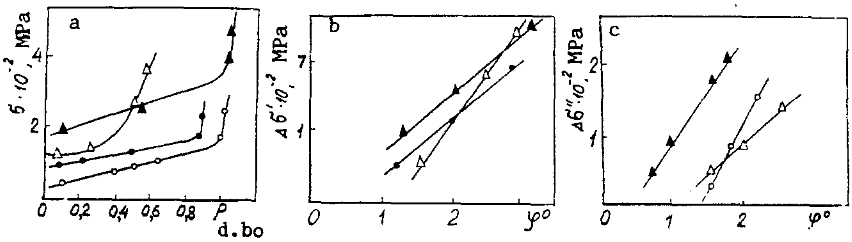

Fig. 7. Influence of the parameters characterizing the disorientations on the boundaries of the cells, on the shearing strength and the additional contributions to $\Delta\sigma'$ and $\Delta\sigma''$. The alloys are Cu—Al and Cu—Mn (see their designations in Fig. 6).

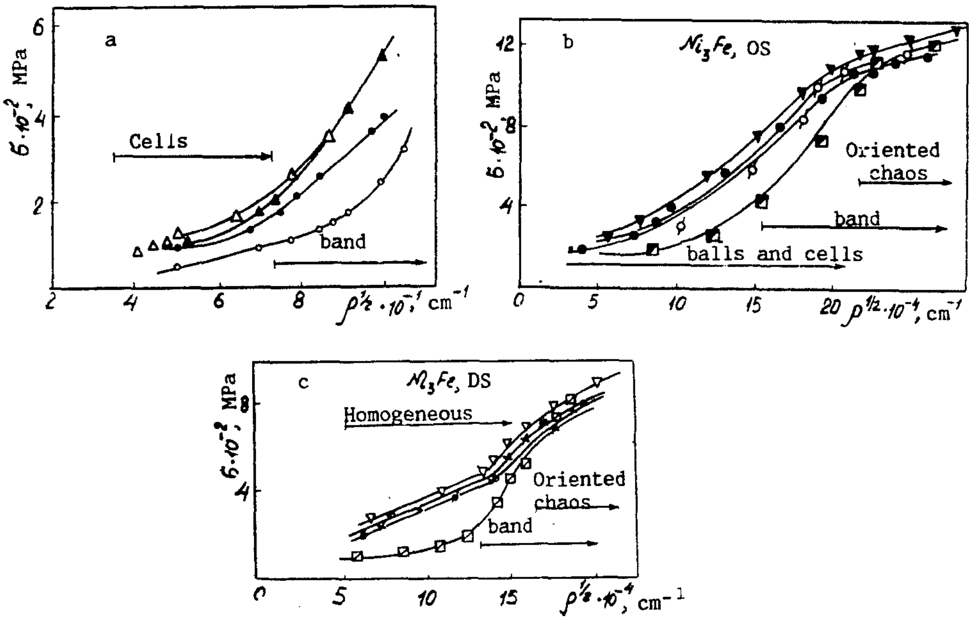

Fig. 8. Dependence of the flow stress σ on $\rho^{1/2}$ in different alloys. The alloys are Cu—Al, Cu—Mn (a), Ni_3Fe (b, c). See the designations of the alloys in Figs. 5 and 6. OS is the ordered state, DS the disordered one.

Band Substructure and Substructure with Continuous and Discrete Disorientations. In these substructures, discrete disorientations on subboundaries can be evaluated by the overall density of the subboundaries M and the angle ω of disorientation on them. Furthermore, in these substructures, there are present distributed dislocated charges, characterizing the mean value of the local excess dislocation density $\rho_{\pm}$, and there is properly a curvature-torsion of the crystal lattice κ. It is clear that here, to the contact retardation of dislocations inside the bands and to the barrier on the boundaries of the band substructure is added yet a contribution of the long-range stress fields. Let us consider in detail the factors here determining the flow stress.

In Fig. 8 are represented the dependences $\sigma = f(\rho^{1/2})$ for alloys in which the formation is observed of band substructure after the disoriented cellular one (for alloys on the basis of copper, Fig. 8a [16]), and for alloys in which not only a band substructure is observed, but also a substructure following after it was continuous and discrete disorientations (for alloys based on nickel, Fig. 8b, c [12, 19, 30]). The formation of the band substructure entails the increase of the parameter $m\alpha$ (in the case of monocrystals — α). The appearance and development of the substructure of organized chaos (b, c) leads to a certain lowering of the value of $m\alpha$.

With the growth of disorientation in the substructure, resistance to deformation also grows (Fig. 9) [12, 30, 40]. In nickel alloys with a band substructure, the dependence of the flow stress on the density of the boundaries (M) of the band substructure, the excess

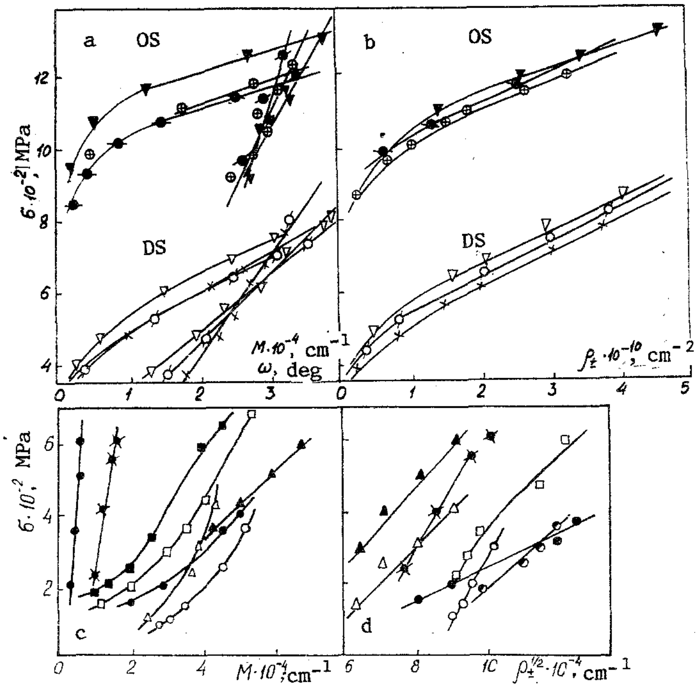

Fig. 9. Connection of the flow stress with the parameters of the band substructure; a, b are alloys based on nickel; c, d are copper. The designations of the alloys are in Figs. 5 and 6.

dislocation density ($\rho_{\pm}$) and the curvature-torsion ($\varkappa$) of the crystal lattice has a nonlinear character, and for alloys with substructural oriented chaos, a linear one (Figs. 9a, b). The dependence on the angle of disorientation is linear for both substructures. In the part of the copper alloys with a band substructure, there is also a departure of $\sigma = f(M)$ from linearity (Fig. 9c). In Fig. 9d $\sigma = f(\rho_{\pm}{}^{1/2})$ is represented for copper alloys. The basis for such a representation is the sufficiently homogeneous distribution of excess dislocation density according to the volume of the band substructure. The linear character of $\sigma = f(\rho_{\pm}{}^{1/2})$ testifies to the fact that the dislocated structure is according to its configuration close to a Strunin ensemble [41]. Oppositely, the linear connection of σ and ρ_{+} testifies to a location of the dislocations similar to that which is considered [42] in the Ryaboshapka–Masyukevich ensemble (localized dislocated charges).

Discussing the role of the excess dislocation density and the long-range stress fields, it is necessary to note that, first, to separate the effects of barrier retardation and retardation caused by long-range stress fields (these are proportional either to κ and $\rho_{\pm}$, or $\rho_{\pm}{}^{1/2}$ depending on the type of dislocation ensemble) is presently not possible, and second, that the sources of the long-range stress fields are not only distributed excess dislocations, but also imperfect ones with variable disorientation and ragged subboundaries [43, 44], and also junctures of grains and ledges on their boundaries in polycrystals [20, 29,36].

The additional contribution $\Delta\sigma$ (see Fig. 2) caused by the transition to disoriented substructures, in the majority of cases linearly depends both on the density of band boundaries and on $\rho_{\pm}$ or $\rho_{\pm}{}^{1/2}$ (Fig. 10). Such dependence emphasizes that the change of the effectiveness of the displacement retardation in passing to a band substructure and a substructure with continuous and discrete orientations (growth of $m\alpha$) is incumbent upon retardation on the subboundaries and the contribution of the long-range stress fields.

Attempts to evaluate it have been undertaken by several methods [14, 30, 36]. Apparently, the most adequate is the direct measurement of the curvature-torsion of the crystal lattice by the electron microscopy method on thin foils using kinked extinct contours [20, 29, 36] and a subsequent computation according to these data of the contributions of long-range stress fields by a model of a suitable dislocation ensemble. Such estimates show that this contribution attains 1/4-1/3 from the acting stresses.

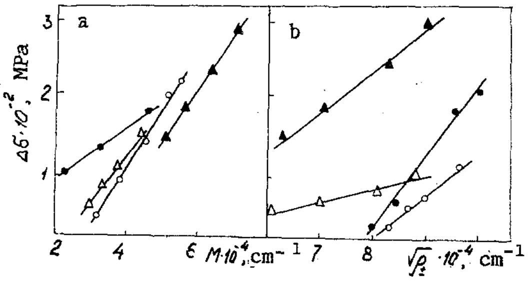

Fig. 10. Contribution $\Delta\sigma$, caused by disorientation, as a function of the parameters of the band substructure and substructure of oriented chaos. The alloys based on copper (the designations of the alloys are in Fig. 6): M is the density of the subboundaries, $\rho_\pm$ is the excess dislocation density.

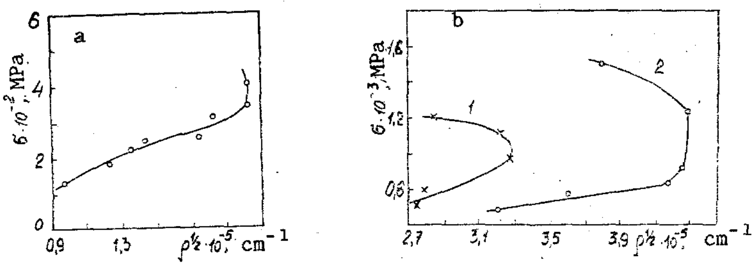

Fig. 11. Dependence of the flow stress on the scalar dislocation density in monocrystals of nickel with orientation [011] (a) and in two (1, 2) chrome-nickel steels of different concentration (b).

Fragmented Substructure. By the measure of development of this substructure, dislocations uniformly distributed inside the fragments annihilate or leave on the boundaries, and the dislocation density at first starts to grow, and then diminishes [13, 44]. Simultaneously, the perfection of the boundaries of the fragments grows and the long-range stress fields lessen. Therefore, with the development of substructure, only the barrier retardation caused by the subboundaries is maintained and grows.

In Fig. 11 are represented the dependences $\sigma = f(\rho^{1/2})$ for monocrystal Ni and alloyed chrome-nickel steel, in which at a high dislocation density a fragmented substructure is formed, while in monocrystals of Ni it attains less perfection. In the figure a sharp departure from the linearly increasing dependence $\sigma = f(\rho^{1/2})$, which appears in the origin of the band substructure is clearly apparent. The characteristic downturn and subsequent reverse course of this dependence is connected with the appearance of fragmented substructure. In its ideal development it was related by us in the survey [8] to a dislocation-free one. For a fragmented substructure, an inversely proportional dependence of the flow stress on the mean dimension of the fragments D_F is observed (Fig. 12 a, b). (The dimension of the fragments D_F and the density of their boundaries $P_{bo.F}$ are inversely proportional to each other $D_F^{-1} \sim P_{bo.F}$.) In the literature [13, 38] either the dependence $\sigma \sim D_F^{-1}$ or $\sigma \sim D_F^{-1/2}$ is observed. In our papers the additional contribution $\Delta\sigma$, caused by the fragmentation, proves to be approximately proportional to the density of boundaries of the fragments $P_{bo.F}$ (Fig. 12c). In this manner, on hand is a proof that the basic contribution to the field stress in this substructure is the barrier retardation.

Twin Substructure. The inclusion of twinning in deformation on the basis of a developed dislocation substructure naturally alters the dependence $\sigma = f(\rho^{1/2})$. Moreover, the value of the parameter $m\alpha$ grows [45], and the parameter itself partially loses physical sense and can be considered as effective. In Fig. 13a is represented the dependence $\sigma = f(\rho^{1/2})$ for a number of alloys, in which twinning begins not with the very start of deformation, but only for the attainment of some critical hardening. The contribution $\Delta\sigma$, caused by twinning (the method of determining it is indicated in Fig. 2b) is linearly connected with the density of twins P_{TW} (Fig. 13b) which also cause barrier retardation.

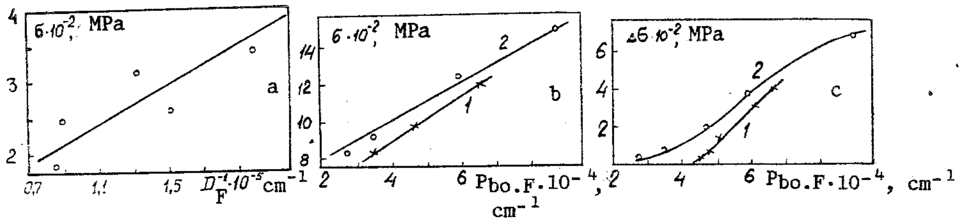

Fig. 12. Proportionality of the flow stress and the additional contribution $\Delta\sigma$ of the density of the boundaries of the fragments: a) monocrystals of nickel; b, c) chrome–nickel steel.

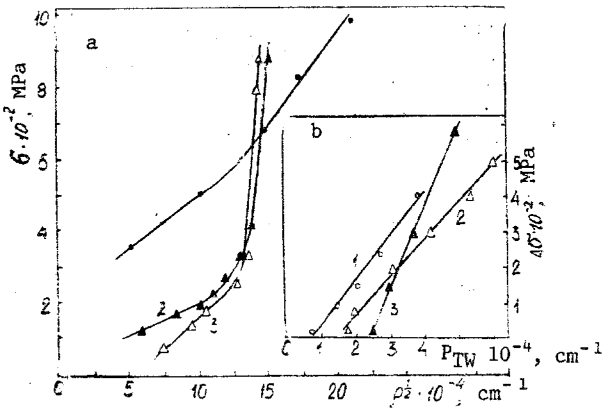

Fig. 13. Resistance to deformation in twinned substructure: a) the dependence $\Delta\sigma = f(\rho^{1/2})$; b) $\Delta\sigma = f(P_{TW})$; 1 are polycrystals of steel Fe–Mn; 2) Cu + 10 at. % Al; 3) Cu + 14 at. % Al.

Substructure with Deformed Martensite. In our papers have been conducted special investigations on iron alloys with an unstable crystal lattice selected in such a manner that α- or ε-martensite form after a specified degree of deformation, which is implemented by slippage. The observable dependence $\sigma = f(\rho^{1/2})$ is, in this case, similar to that which occurs in twinning following after slippage. In the formation of martensite, the effective value of the parameter $m\alpha$ also increases. The additional contribution $\Delta\sigma$, caused by deformed martensite proves in the majority of cases to be proportional to the density of bands of ε-martensite or the volume fraction of α-martensite. The contribution has a barrier nature.

CONCLUSIONS

In one-phase metallic materials, the stress flow is determined by the contributions of the substructural hardening σ_{su}, the solid-solution σ_{ss}, the lattice σ_{lat}, and a contribution connected with the presence of boundaries of grains σ_p (a contribution of Hall–Petch type in polycrystals):

$$\sigma = \sigma_{su} + \sigma_{ss} + \sigma_{lat} + \sigma_p . \tag{2}$$

Substructural hardening, in its turn, can be represented (in an additive approximation) in the following manner:

$$\sigma_{su} = \Delta\sigma_c + \Delta\sigma_{bar} + \Delta\sigma_\ell + \Delta\sigma_{FL} . \tag{3}$$

Here $\Delta\sigma_c$ is a contribution caused by retardation on dislocations distributed in the volume of the material (contact retardation). For this contribution, the connection with the dislocation density is expressed by formula (1). The next contribution $\Delta\sigma$ is the barrier retardation. Depending on the type of substructure, displacement retardation occurs on the dislocation concentrations, the boundaries of the cells, the subboundaries, and the boundaries of the fragments (see Fig. 1). This contribution is expressed by the relations

$$\Delta\sigma_{bar} \sim L^{-1},\ \Delta\sigma_{bar} \sim D^{-1},$$
$$\Delta\sigma_{bar} \sim M^{-1},\ \Delta\sigma_{bar} \sim D_F^{-1}, \tag{4}$$

TABLE 2. Hardening Caused by Different Classes of Substructures

Classes of substructures	Basic contributions to resistance to deformation	Defining relations	Parameters of the substructure, controlling shearing strength
Homogeneous nondisoriented	Contact retardation $\Delta\sigma_c$	$\Delta\sigma_c = m\alpha Gb\rho^{1/2}$	Scalar dislocation density ρ
Inhomogeneous nondisoriented	Contact and (or) barrier retardation $\Delta\sigma_c + \Delta\sigma_{bar}$	$\Delta\sigma_c \sim \rho_{co}{}^{1/2}$ $\Delta\sigma_c \sim \rho_{wa}{}^{1/2}$,	Dislocation density in concentrations ρ_{co} and in walls of cells ρ_{wa}
		$\Delta\sigma_{bar} = K'/L$, $\Delta\sigma_{bar} = K''/D$	Distance between concentrations L and dimension of cells D
Inhomogeneous disoriented	Contact and (or) barrier retardation and long-range stress fields $\Delta\sigma_c + \Delta\sigma_{bar} + \Delta\sigma_\ell$	$\Delta\sigma_c \sim \rho_{co}{}^{1/2}$; $\Delta\sigma_c \sim \rho_{wa}{}^{1/2}$, $\Delta\sigma_{bar} = K'/L$; $\Delta\sigma_{bar} = K''/D$ $\Delta\sigma_{bar} \sim P_{d.bo}$ $\Delta\sigma_{bar} \sim \varphi$, $\Delta\sigma_\ell \sim \rho_\pm$ or $\rho_\pm{}^{1/2}$	ρ_{wa}, ρ_{co} L, D Density of disoriented boundaries of cells $P_{d.bo}$. The angle of disorientation on the boundaries of the cells φ. Excess dislocation density.
Disoriented dislocation-disclination	Contact and barrier retardation and long-range stress fields $\Delta\sigma_c + \Delta\sigma_{bar} + \Delta\sigma_\ell$	$\Delta\sigma_{bar} \sim M$, $\Delta\sigma_{bar} \sim \omega$,	Density of subboundaries M and disorientation ω on them Excess dislocation density $\rho_\pm$.
		$\Delta\sigma_\ell \sim \rho_\pm$ or $\rho_\pm{}^{1/2}$ $\Delta\sigma_\ell \sim \varkappa$	Curvature-torsion of crystal lattice $\varkappa$
Disoriented dislocation-free	For nonideal fragmented $\Delta\sigma_{bar}$	$\Delta\sigma_{bar} \sim D_F{}^{-1}$	Dimension of fragments D_F
Nonideal fragmented	For nonideal fragmented $\Delta\sigma_{bar} + \Delta\sigma_\ell$	$\Delta\sigma_p \sim T$, $\Delta\sigma_\ell \sim \varkappa$	Density of ragged subboundaries T. Curvature-torsion of crystal lattice $\varkappa$
Twinning	Barrier retardation and long-range stress fields $\Delta\sigma_{bar} + \Delta\sigma_\ell$	$\Delta\sigma_{bar} \sim P_{TW}$ $\Delta\sigma_\ell \sim \varkappa$	Density of twins P_{TW} Curvature-torsion of crystal lattice $\varkappa$
Martensitic	Barrier and contact retardation and long-range stress fields $\Delta\sigma_{bar} + \Delta\sigma_c + \Delta\sigma_\ell$	$\Delta\sigma_{bar} \sim P_\varepsilon$, $\Delta\sigma_{bar} \sim \Delta V_\alpha$, $\Delta\sigma_\ell \sim \varkappa$	Density of plates of ε-martensite P_ε. Volume share of α-martensite ΔV_α. Curvature-torsion of crystal lattice $\varkappa$

respectively, describing the cellular-reticular, cellular, band, and fragmented substructures. The third contribution is the long-range stress fields. Depending on the type of dislocation ensemble, it has the form

$$\Delta\sigma_\ell \sim \rho_\pm^{1/2} \quad \text{or} \quad \Delta\sigma_\ell \sim \rho_\pm. \tag{5}$$

The fluctuation correction $\Delta\sigma_{FL}$ is caused by the inhomogeneous distribution of dislocations in the volume of the material. It is discussed in detail in [7]. The corresponding expression has the form

$$\Delta\sigma_{FL} = -\frac{m\alpha}{8} Gb\rho^{-3/2} M_2(\rho), \tag{6}$$

where $M_2(\rho)$ is the second moment of the distribution function of dislocation density. In distinction from the others, this contribution has a negative sign, since the slippage develops in the least-hardened regions of the material. Similar contributions caused by the inhomogeneous distribution of boundaries of cells or subboundaries and dislocation charges, also occur. Apparently, in complicated substructures it is necessary to find a fluctuation correction caused by the spatial fluctuation of the contributions from all the simultaneously active hardening mechanisms.

The nature of substructural hardening is presented in generalized form in Table 2 in correspondence with the basic types of substructures.

In conclusion the authors consider it a pleasant duty to express gratitude to their students and collaborators. A number of original results, presented in the article, were obtained through the efforts of senior scientific collaborators, L. I. Trishkina, N. A. Popov, A. V. Paul', G. L. Fedoseev, L. N. Ignatenko, T. S. Kunitsyna, O. B. Perevalova, N. V. Girsov, and assistant S. P. Zhukovskii. In the formulation of a number of concepts presented in the article, the docents L. A. Teplyakova, D. V. Lychagin, Yu. P. Sharkeev, V. A. Starenchenko, I. A. Lapsker, and Yu. A. Abzaev took part.

LITERATURE CITED

1. Mechanisms of Strengthening Solids [in Russian], M. L. Bernshtein (ed.), Metallurgiya, Moscow (1965).
2. Strengthening Methods in Crystals, Applied Science Publishers Ltd, London (1971).
3. L. E. Popov, V. C. Kobytev, and T. A. Kovalevskaya, Plastic Deformation of Alloys [in Russian], Metallurgiya, Moscow (1984).
4. F. Nabarro, R. N. Bazinskii, and D. V. Kholt, The Plasticity of Monocrystals [in Russian], Metallurgiya, Moscow (1967).
5. V. I. Trefilov, Yu. V. Mil'man, and S. A. Firstov, Physical Bases of Strength of Refractory Metals [in Russian], Naukova Dumka, Kiev (1975).
6. L. E. Popov, V. S. Kobytev, and L. V. Ganzya, The Theory of Deformed Strengthening of Alloys [in Russian], Tomsk State University Press, Tomsk (1981).
7. N. A. Koneva and É. V. Kozlov, Izv. Vyssh. Uchebn. Zaved., Fiz., No. 8, 3-14 (1982).
8. N. A. Koneva and É. V. Kozlov, Izv. Vyssh. Uchebn. Zaved., Fiz., No. 2, 89-106 (1990).
9. N. A. Koneva, S. P. Zhukovskii, I. A. Lapsker, and É. V. Kozlov, Physics and Electronics of a Solid [in Russian], No. 5, Udmurt State University Press, Izhevsk (1982), pp. 88-97.
10. Yu. P. Sharkeev, I. A. Lapsker, N. A. Koneva, and É. V. Kozlov, Fiz. Met. Metalloved., 60, No. 4, 816-821 (1985).
11. N. A. Koneva, S. P. Zhukovskii, I. A. Lapsker, et al., in: Physics of Defects of Surface Layers of Materials [in Russian], A. F. Ioffe Physico-Technical Institute, Leningrad (1989), pp. 113-131.
12. N. A. Koneva, D. V. Lychagin, L. A. Teplyakova, and É. V. Kozlov, in: Theoretical and Experimental Analysis of Disclinations [in Russian], A. F. Ioffe Physico-Technical Institute, Leningrad (1986), pp. 116-126.
13. V. A. Likhachev, V. E. Panin, E. É. Zasimchuk, et al., Cooperative Deformation Processes and Localization of Deformation [in Russian], Naukova Dumka, Kiev (1989).
14. N. A. Koneva, L. A. Teplyakova, and É. V. Kozlov, in: Structure and Plastic Behavior of Alloys [in Russian], Tomsk State University Press, Tomsk (1983), pp. 74-99.
15. N. A. Koneva, D. V. Lychagin, L. I. Trishkina, and E. V. Kozlov, in: Strength of Metals and Alloys, Vol. 1, Proceedings of the ICSMA-7, Montreal, Canada, August 12-16, 1985, Pergamon, London (1985), pp. 21-26.
16. N. A. Koneva, L. I. Trishkina, G. V. Daneliya, et al., Fiz. Met. Metalloved., 66, No. 4, 808-813 (1988).
17. V. N. Gridnev, V. I. Trefilov, S. A. Firstov, et al., Phase and Structural Transformations and Metastable States in Metals [in Russian], Naukova Dumka, Kiev (1988).

18. N. A. Koneva, G. A. Perov, L. E. Popov, et al., Izv. Vyssh. Uchebn. Zaved., Fiz., No. 2, 94-98 (1982).
19. N. A. Koneva, L. A. Teplyakova, D. V. Lychagin, et al., in: Strength of Metals and Alloys, Vol. 1, Proceedings of the ICSMA-7, Montreal, Canada, August 12-16, 1985, Pergamon, London (1985), pp. 27-31.
20. N. A. Koneva, É. V. Kozlov, L. I. Trishkina, and D. V. Lychagin, in: Papers of the International Conf., May 26-31, 1990, Terskol (USSR), Tomsk State University Press, Tomsk (1990), pp. 83-93.
21. A. Howie, in: The Proceedings of the European Conference on Electron Microscopy, Vol. 1, De Nederlands Verenigung voor Electronenmicroscopie, Delft (1960), pp. 383-386.
22. A. Howie, in: Direct Observation of Imperfections in Crystals [Russian translation], Metallurgiya, Moscow (1964), pp. 198-208.
23. N. A. Koneva, D. V. Lychagin, L. A. Teplyakova, and É. V. Kozlov, in: Experimental Investigation and Theoretical Description of Disclinations [in Russian], A. I. Ioffe Physico-Technical Institute, Leningrad (1984), pp. 161-167.
24. N. A. Koneva, D. V. Lychagin, S. P. Zhukovskii, and É. V. Kozlov, Fiz. Met. Metalloved., 60, No. 1, 171-179 (1985).
25. N. A. Koneva, D. V. Lychagin, O. B. Perevalova, et al., in: Plastic Deformation of Alloys [in Russian], Tomsk State University Press, Tomsk (1986), pp. 120-132.
26. L. I. Trishkina and E. V. Kozlov, in: Substructure and Mechanical Properties of Metals and Alloys [in Russian], Tomsk Polytechnic Institute, Tomsk (1988), pp. 5-11.
27. N. A. Koneva, Doctoral Dissertation, Tomsk (1988).
28. A. V. Paul' and N. A. Koneva, in: Substructure and Mechanical Properties of Metals and Alloys [in Russian], Tomsk Polytechnic Institute, Tomsk (1988), pp. 20-26.
29. N. A. Koneva, D. V. Lychagin, L. I. Trishkina, and É. V. Kozlov, in: Physical Aspects of Prediction of Destruction and Deformation of Heterogeneous Materials [in Russian], A. F. Ioffe Physico-Technical Institute, Leningrad (1987), pp. 20-36.
30. N. A. Koneva, D. V. Lychagin, L. A. Teplyakova, and E. V. Kozlov, in: Strength of Metals and Alloys, Vol. 1, Proceedings of the JCSMA-8, Tampere, Finland, August 22-26, 1988, Pergamon, London (1988), pp. 385-390.
31. Yu. P. Sharkeev, É. V. Kozlov, and N. A. Koneva, in: Strengthening of Atoms and Properties of Alloys [in Russian], Naukova Dumka, Kiev (1979), pp. 254-256.
32. T. S. Kunitsyna, L. A. Teplyakova, and N. A. Koneva, in: Dislocational Structure in Metals and Alloys and Methods for Investigating It [in Russian], Tula Polytechnic Institute, Tula (1987), pp. 19-23.
33. T. S. Kunitsyna and N. A. Koneva, in: Defects and Physical-Mechanical Properties of Metals and Alloys [in Russian], Altai Krai Polytechnic Institute Press, Barnaul (1987), pp. 103-108.
34. Yu. A. Abzaev, V. A. Starenchenko, N. A. Koneva, and É. V. Kozlov, Izv. Vyssh. Uchebn. Zaved., Fiz., No. 3, 65-70 (1987).
35. A. Zeeger, in: Dislocations and Mechanical Properties of Crystals [Russian translation], Inostr. Lit., Moscow (1960), pp. 179-289.
36. É. V. Kozlov, D. V. Lychagin, N. A. Popova, et al., in: Physics of Durability of Heterogeneous Materials [in Russian], A. F. Ioffe Physico-Technical Institute, Leningrad (1988), pp. 3-13.
37. M. R. Staker and H. Holt, Acta. Met., 20, No. 4, 569-579 (1972).
38. V. I. Trefilov, V. F. Moiseev, E. P. Pechkovskii, et al., Deformational Strengthening and Destruction of Polycrystalline Metals [in Russian], Naukova Dumka, Kiev (1989).
39. S. Kawasaki and T. Takeuchi, Scr. Met., 14, No. 2, 183-188 (1980).
40. N. A. Koneva, D. V. Lychagin, L. A. Teplyakova, et al., in: Disclinations and Rotational Deformation of Solids [in Russian], A. F. Ioffe Physico-Technical Institute, Leningrad (1988), pp. 103-113.
41. B. M. Strunin, Fiz. Tverd. Tela, 9, No. 3, 805-812 (1967).
42. A. M. Masyukevich and K. P. Ryaboshapka, Metallofizika, No. 63, 23-27 (1976).
43. V. I. Vladimirov and A. E. Romanov, Disclinations in Crystals [in Russian], Nauka, Leningrad (1986).
44. V. Rybin, Large Plastic Deformations and the Destruction of Metals [in Russian], Metallurgiya, Moscow (1986).
45. N. A. Popova and I. A. Lapsker, in: Plastic Deformation of Alloys [in Russian], Tomsk State University Press, Tomsk (1986), pp. 204-248.